ISSN 0915-633X

NATIONAL INSTITUTE FOR FUSION SCIENCE

A New Technique Based on the Transformation of Variables for Nonlinear Drift and Rossby Vortices

K. Orito

(Received - July 3, 1996)

NIFS-424 July 1996

RESEARCH REPORT
NIFS Series

NAGOYA, JAPAN

A New Technique Based on the Transformation of Variables for Nonlinear Drift and Rossby Vortices

Kohtaro ORITO* **

Department of Physics, Nagoya University, Nagoya 464-01

(Received July 4, 1996)

The quasi-two-dimensional nonlinear equations for drift and Rossby vortices have some stationary multipole solutions, and especially the dipole vortex solution is called modon. These solutions are valid only in the lowest order where the fluid velocity has a stream function. In order to investigate features of the multipole solutions more accurately, the effect of the higher order terms, for example the polarization drift in a plasma or the Coriolis force in a rotating planet, needs to be considered. It is shown that the higher order analysis through a new technique based on a transformation of variables is much easier than a straightforward iteration. The solutions in this analysis are obtained by inverse transformation to the original coordinates, where the profiles of potentials are distorted by the effects of higher order terms.

KEYWORDS: drift vortex, Rossby vortex, potential vorticity, Hasegawa-Mima equation, modon, monopole vortex

* Email address: orito@sriran.nifs.ac.jp

** Present address: National Institute for Fusion Science, Nagoya 464-01, Japan

§1. Introduction

The Hasegawa-Mima (H-M) equation[1] is one of the simplest and successful equations that describe nonlinear drift vortices in inhomogeneous and magnetized plasmas in quasi-two-dimension. The solution of the H-M equation obtained by Larichev and Reznik has the profile of a localized dipole vortex, the so-called modon, in the plane perpendicular to the uniform magnetic field $\boldsymbol{B}_0$.[2] Modons propagate stably in the direction of the electron diamagnetic flow with the constant phase velocity.

Recently, the incorporation of the effects of the shear flow or the magnetic shear, which are not included in the H-M equation, have been discussed.[3-5] This means mathematically to add higher order quantities into the H-M equation. The polarization drift is also one of higher order effects and important when we consider the temporal evolution of the nonlinear drift vortex. However, if the effect of the polarization drift is taken into consideration, it is very difficult to solve the nonlinear drift equation analytically or even on a computer. The main subject of the present paper is to show how to avoid the difficulty and to solve the equation in a simpler way.

The Charney equation for a nonlinear Rossby vortex in planetary atmosphere is similar to the H-M equation in plasma physics and is also obtained in the lowest order nonlinearities.[6] Orito, Sato and Irie[7] have derived an equation including higher order terms by using a transformation of variables in the long wavelength ordering, that is $\rho_0^2\nabla^2 \ll 1$, where ρ_0 is the Rossby radius. In the present paper we apply the transformation of variables to various cases.

In Sections 2 and 3, we derive the basic equations for the drift vortex and the Rossby vortex, respectively, and the conservation law of the potential vorticity which is common in both cases. The transformation of variables is introduced in Sec. 4 and is applied to nonlinear equations, which we cannot solve analytically, for the drift wave in the short wavelength ordering and the Rossby wave in the short/long wavelength ordering in Sec. 5. The conclusion and discussions are given in Sec. 6.

§2. Nonlinear Drift Vortices

We assume that there is an inhomogeneous cold ion plasma in a uniform magnetic field and that the electric field is described by an electrostatic potential, that is $T_i = 0$, $\boldsymbol{B}_0 = B_0\hat{\boldsymbol{z}}$, and $\boldsymbol{E} = -\nabla\phi$. In this situation, the drift wave propagates toward the y direction with the drift velocity which is proportional to the unperturbed density gradient in the x direction. For simplicity, we introduce dimensionless variables by $\boldsymbol{r}/\rho_s \to \boldsymbol{r}$, $\omega_{ci}t \to t$, $e\phi/T_0 \to \phi$, where $\rho_s = c_s/\omega_{ci}$, $c_s = \sqrt{T_0/m}$, $\omega_{ci} = eB_0/m$, in which m and e are the ion mass and charge and T_0 is the electron temperature, respectively. The equations of motion and continuity for ions are given by

$$\frac{\partial \boldsymbol{v}}{\partial t} + (\boldsymbol{v}\cdot\nabla)\boldsymbol{v} = -\nabla\phi + \boldsymbol{v}\times\hat{\boldsymbol{z}}, \tag{2.1}$$

$$\frac{\partial n}{\partial t} + \nabla \cdot (n\boldsymbol{v}) = 0, \tag{2.2}$$

where $\boldsymbol{v}$ and n are the velocity and the density of ions, respectively. Making the usual assumptions that electrons take the Boltzmann distribution and plasmas are quasineutral. we obtain

$$n = n_0(x)\exp(\phi), \tag{2.3}$$

where the equilibrium density $n_0(x)$ assumes the form $\ln n_0(x) = \nu_0 x$. Substituting eq. (2.2) into the curl of eq. (2.1), we obtain the following conservation law,

$$\left(\frac{\partial}{\partial t} + \boldsymbol{v} \cdot \nabla\right) q = 0, \tag{2.4}$$

$$q = \ln\left(\frac{1+\Omega}{n}\right), \tag{2.5}$$

where Ω means the z component of the vorticity, $\Omega = \hat{\boldsymbol{z}} \cdot \nabla \times \boldsymbol{v}$, and q is called the generalized vorticity or the potential vorticity.

In the short wavelength region, we introduce the following ordering with the smallness parameter ϵ,

$$\epsilon \sim \frac{\partial}{\partial t} \sim \boldsymbol{v} \cdot \nabla \sim \Omega \sim \frac{|\nabla \ln n_0|}{|\nabla \ln \phi|}. \tag{2.6}$$

In addition, the dimensionless electrostatic potential ϕ is regarded as of order ϵ, because the electrostatic potential is much less than the electron kinetic energy. The velocity $\boldsymbol{v}$ in eq. (2.4) is defined as the sum of the $E \times B$ drift $\boldsymbol{v}_E$ and the polarization drift $\boldsymbol{v}_p$ by iteration of eq. (2.1) up to third order in ϵ, where

$$\boldsymbol{v}_E = \hat{\boldsymbol{z}} \times \nabla\phi \tag{2.7}$$

and

$$\boldsymbol{v}_p = -\left(\frac{\partial}{\partial t} + \boldsymbol{v}_E \cdot \nabla\right)\nabla\phi. \tag{2.8}$$

In the lowest order $\boldsymbol{v} = \boldsymbol{v}_E$, we obtain the H-M equation,

$$\frac{\partial q}{\partial t} + \{\phi, q\} = 0, \tag{2.9}$$

$$q = \nabla^2\phi - \phi - \nu_0 x, \tag{2.10}$$

where the bracket in the second term on the left hand side is the Poisson bracket with respect to x and y, and the expression of q is valid to the first order in eq. (2.5). It is known that the H-M equation (2.9) has some multipole solutions, especially the modon.

When we take the convection term $\boldsymbol{v} \cdot \nabla q$ up to the second order in ϵ, we obtain

$$\frac{\partial q}{\partial t} - \frac{\partial \nabla\phi}{\partial t} \cdot \nabla q - \nabla^2\phi\{\phi, q\} + \{\phi + (\nabla\phi)^2/2, q\} = 0. \tag{2.11}$$

It is difficult to solve analytically such equation including the effect of the polarization drift which has higher derivatives and nonlinear terms. It is shown how we solve this problem in Sections 4 and 5.

§3. Nonlinear Rossby Vortices

We consider the quasi-two-dimensional barotropic fluid on a rotating planet. We adopt local orthogonal coordinates on a certain latitude θ_0 of the northern hemisphere with the x-axis toward north, the y-axis west and z-axis local zenith. The fluid on the planet receives the gravity $-g\nabla H$ and the Coriolis force $f(x)\boldsymbol{v} \times \hat{\boldsymbol{z}}$, where the depth of fluid is $H(x,y) = H_0(1 + h(x,y))$ and the Coriolis parameter $f(x) = f_0 + f_1 x + f_2 x^2/2$, in the so-called β-plane approximation. We introduce dimensionless variables by $\boldsymbol{r}/\rho_0 \to \boldsymbol{r}$, $f_0 t \to t$ and $f(x)/f_0 \to f(x) = 1 + \beta_1 x + \beta_2 x^2/2$, where $\rho_0 = \sqrt{gH_0}/f_0$, $\beta_1/\rho_0 = f_1/f_0 = \mu\cot\theta_0$ and $\beta_2/\rho_0 = f_2/f_0 = -\mu^2$ with $\mu = \rho_0/R_p$ and R_p is the planet radius. The basic equations of motion and continuity in the dimensionless form are given by

$$\frac{\partial \boldsymbol{v}}{\partial t} + (\boldsymbol{v}\cdot\nabla)\boldsymbol{v} = -\nabla h + f(x)\boldsymbol{v} \times \hat{\boldsymbol{z}}, \tag{3.1}$$

$$\frac{\partial h}{\partial t} + \nabla\cdot[(1+h)\boldsymbol{v}] = 0, \tag{3.2}$$

where $\boldsymbol{v}$ is the fluid velocity in the two-dimensional x-y plane. From eqs. (3.1) and (3.2), we derive the conservation law of the potential vorticity q, which is similar to eq. (2.4) with eq. (2.5),

$$\left(\frac{\partial}{\partial t} + \boldsymbol{v}\cdot\nabla\right) q = 0, \tag{3.3}$$

$$q = \frac{f(x) + \Omega}{1+h}, \tag{3.4}$$

where the vorticity is $\Omega = \hat{\boldsymbol{z}}\cdot\nabla\times\boldsymbol{v}$.

We define the short wavelength ordering in terms of a smallness parameter ϵ by

$$\epsilon \sim \frac{\partial}{\partial t} \sim \boldsymbol{v}\cdot\nabla \sim \Omega \sim h \sim \frac{|\nabla \ln f|}{|\nabla \ln h|}. \tag{3.5}$$

The velocity obtained by iteration of eq. (3.1) is

$$\boldsymbol{v} = \boldsymbol{v}_l + \boldsymbol{v}_\beta + \boldsymbol{v}_h, \tag{3.6}$$

where

$$\boldsymbol{v}_l = \hat{\boldsymbol{z}} \times \nabla h, \tag{3.7}$$

$$\boldsymbol{v}_\beta = -\beta_1 x\, \hat{\boldsymbol{z}} \times \nabla h \tag{3.8}$$

and

$$\boldsymbol{v}_h = -\left(\frac{\partial}{\partial t} + \boldsymbol{v}_l\cdot\nabla\right)\nabla h. \tag{3.9}$$

Here $\boldsymbol{v}_l$ is of the order of ϵ, while both $\boldsymbol{v}_\beta$ and $\boldsymbol{v}_h$ are of the order of ϵ^2. In the lowest order $\boldsymbol{v} = \boldsymbol{v}_l$, we obtain a following equation from eq. (3.3),

$$\frac{\partial q}{\partial t} + \{h, q\} = 0, \tag{3.10}$$

$$q = \nabla^2 h - h + \beta_1 x. \tag{3.11}$$

These equations are the same form as the H-M equation (2.9) with eq. (2.10) if ϕ and $-\nu_0$ are exchanged for h and β_1, respectively.

Since the lowest velocity $\boldsymbol{v}_l$ is independent of the latitude θ_0, we should take account of the effect of the higher velocity $\boldsymbol{v}_\beta$ including the Coriolis parameter β_1 which is proportional to cotθ_0. The other higher order velocity $\boldsymbol{v}_h$ is similar to the polarization drift in plasmas and important in the temporal evolution. Substituting $\boldsymbol{v} = \boldsymbol{v}_l + \boldsymbol{v}_\beta + \boldsymbol{v}_h$ into eq. (3.3), we obtain a generalized nonlinear equation. However, it is difficult to solve it in the same reason as in case of eq. (2.11).

In the long wavelength ordering, we redefine the smallness parameter ϵ as

$$\begin{aligned} \frac{\partial}{\partial t} \sim \boldsymbol{v}\cdot\nabla \sim \Omega \quad &\sim \quad \epsilon^2, \\ h \sim |\nabla \ln f|/|\nabla \ln h| \quad &\sim \quad \epsilon. \end{aligned} \tag{3.12}$$

In this ordering, $\nabla^2 \sim \epsilon$ so that $\boldsymbol{v}_l \sim \epsilon^{3/2}$, $\boldsymbol{v}_\beta \sim \epsilon^{5/2}$, and $\boldsymbol{v}_h \sim \epsilon^{7/2}$. When the terms of the order of ϵ^5 are negligible, a equation obtained straightforward from eqs. (3.3) is not the same form of eq. (3.10). However, Using $\boldsymbol{v}_\beta \cdot \nabla q = \{h, -\beta_1^2 x^2/2\}$, we obtain eq. (3.10) for the potential vorticity

$$\begin{aligned} q = \nabla^2 h - h + \beta_1 x - \beta_1 x h \\ + h^2 + (\beta_2 - \beta_1^2)x^2/2. \end{aligned} \tag{3.13}$$

In the stationary condition $\partial/\partial t = -u\partial/\partial x$, assuming both h and $\nabla^2 h \to 0$ as $y \to \infty$ at fixed x, we derive

$$\nabla^2 h + \lambda h^2 + \gamma x h - \kappa^2 h = 0, \tag{3.14}$$

where $\lambda = 1 - (\beta_2 - \beta_1^2)/2u^2$, $\gamma = (\beta_2 - \beta_1^2)/u - \beta_1$ and $\kappa^2 = 1 - \beta_1/u$. It is known that this equation has some approximate monopole solutions near the origin. Such monopole solutions are, however, valid only for $r \sim \epsilon$ and not localized, because h oscillates in the region $x < -\kappa^3/\gamma$ and this oscillation bring out the energy forming the vortex, which has been pointed out by Nycander.[7,9,10].

§4. Transformation of Variables

It is easy to derive the stationary dipole solution (5.5) because of a feature of the Poisson bracket in the H-M equation (2.9). The Poisson bracket means the convective derivative $\boldsymbol{v}_E \cdot \nabla q$,where the $E \times B$ drift velocity $\boldsymbol{v}_E$ is described by the stream function, so that we can regard the ion fluid as incompressible. When we take account of the second order terms $\boldsymbol{v}_p$ the fluid is now compressible, and then we cannot derive equations similar to the H-M equation. This situation is same in the case of discussion about the Rossby vortices in the short/long wavelength ordering. In this section, we introduce a set of variables transforming the compressible fluid velocity to an incompressible fluid velocity.

We start with an equation conserving a suitable quantity q in quasi-two-dimension, which is identical to eq. (2.4) or eq. (3.3), as follows:

$$\left(\frac{\partial}{\partial t} + \boldsymbol{v} \cdot \nabla\right) q = 0, \tag{4.1}$$

where $\boldsymbol{v} = \boldsymbol{v}_1 + \boldsymbol{v}_2$ with $\nabla \cdot \boldsymbol{v}_1 = 0$, $\nabla \cdot \boldsymbol{v}_2 \neq 0$ and $|\boldsymbol{v}_1| \gg |\boldsymbol{v}_2|$. The divergence free velocity is described by a stream function, that is $\boldsymbol{v}_1 = \hat{\boldsymbol{z}} \times \nabla\psi_1$. Now we introduce the transformation of variables

$$\begin{cases} \boldsymbol{X} = \boldsymbol{x} + \boldsymbol{\xi}, \\ \tau = t, \\ \Psi = \psi_1 + \psi_2, \end{cases} \tag{4.2}$$

where $\boldsymbol{X}$ is the two dimensional new coordinate vector (X, Y) with the correction $\boldsymbol{\xi} = (\xi, \eta)$ depending on $\boldsymbol{x}$ and t, and Ψ a new stream function with ψ_2 a correction to ψ_1. In this new coordinates, we assume that eq. (4.1) is rewritten as

$$\left(\frac{\partial}{\partial \tau} + J\nabla'\Psi \cdot \nabla'\right) q = 0, \tag{4.3}$$

or

$$\frac{\partial q}{\partial \tau} + \{\Psi, q\}' = 0 \tag{4.4}$$

where

$$J = \begin{pmatrix} 0 & -1 \\ 1 & 0 \end{pmatrix}$$

is used instead of the operator $\hat{\boldsymbol{z}}\times$ and the derivatives in ∇' and the Poisson bracket with the prime are with respect to (X, Y). If $\boldsymbol{\xi}$ and Ψ exist, we can solve eq. (4.3) in the same way as the H-M equation.

The differentials ∂_τ and ∇' in the new coordinates $(\boldsymbol{X}, \tau)$ can be written by using $\boldsymbol{x}$ and t, i. e. $\partial_\tau = \partial_t - (\partial_t\boldsymbol{\xi}) \cdot \nabla$ and $\nabla' = (I - A)\nabla$, where I is a 2×2 unit matrix and

$$A = \begin{pmatrix} \partial_x\xi & \partial_x\eta \\ \partial_y\xi & \partial_y\eta \end{pmatrix}.$$

Therefore, we derive a conserved equation from equation (4.3) as follows:

$$\left(\frac{\partial}{\partial t} + \boldsymbol{v}' \cdot \nabla\right) q = 0, \tag{4.5}$$

with

$$\begin{aligned} \boldsymbol{v}' = &-\frac{\partial\boldsymbol{\xi}}{\partial t} - (\nabla \cdot \boldsymbol{\xi})\, \hat{\boldsymbol{z}} \times \nabla\psi_1 \\ &+ \hat{\boldsymbol{z}} \times \nabla(\psi_1 + \psi_2). \end{aligned} \tag{4.6}$$

When it is compared with eq. (4.1), we obtain

$$\boldsymbol{v}_2 = -\frac{\partial\boldsymbol{\xi}}{\partial t} - (\nabla \cdot \boldsymbol{\xi})\, \hat{\boldsymbol{z}} \times \nabla\psi_1 + \hat{\boldsymbol{z}} \times \nabla\psi_2. \tag{4.7}$$

If we find out $\boldsymbol{\xi}$ and ψ_2 satisfying eq. (4.7), the solution of eq. (4.3) is transformed into ψ_1 by means of the inverse transformation of eqs.(4.2), that is

$$\psi_1(\boldsymbol{x},t) = \Psi(\boldsymbol{x}+\boldsymbol{\xi},t) - \psi_2(\boldsymbol{x},t). \tag{4.8}$$

§5. Applications to Drift and Rossby Vortices

We apply the transformation of variables to the drift and the Rossby vortices in following three examples.

5.1 Example 1: Drift Vortices in the Short Wavelength Ordering

For the drift wave in the short wavelength ordering, the second order term of the velocity, the polarization drift velocity (2.8), is written

$$\boldsymbol{v}_p = -\frac{\partial}{\partial t}\nabla\phi - \nabla^2\phi\,\hat{\boldsymbol{z}}\times\nabla\phi + \frac{1}{2}\hat{\boldsymbol{z}}\times\nabla(\nabla\phi)^2. \tag{5.1}$$

Comparing it with eq. (4.7), we define the transformation of variables as follows:

$$\begin{cases} \boldsymbol{\xi} = \nabla\phi, \\ \Psi = \phi + \dfrac{1}{2}(\nabla\phi)^2. \end{cases} \tag{5.2}$$

Therefore, eq. (2.4) is really transformed to eq. (4.3) in the new coordinates $(\boldsymbol{X},\tau)$. From eqs. (5.2), we obtain the electrostatic potential

$$\phi(\boldsymbol{x},t) = \Psi(\boldsymbol{x}+\nabla\Psi,t) - \frac{1}{2}(\nabla\Psi(\boldsymbol{x},t))^2. \tag{5.3}$$

The potential vorticity q in eq. (4.3) is given by

$$q(\boldsymbol{X},\tau) = \nabla'^2\Psi - \Psi - \nu_0 X. \tag{5.4}$$

A set of eqs. (4.3) and (5.4) agree with the H-M equation (2.9) with (2.10) and has some stationary multipole localized solutions. Hereafter, we obtain the profile of ϕ if the solution Ψ is a dipole solution, the modon[2]. When the wave frame travels westward along y-axis with constant speed u, we obtain

$$\Psi(R,\theta) = \begin{cases} [AJ_1(kR) + \alpha R]\cos\theta & (R \le r_0) \\ BK_1(pR)\cos\theta & (R > r_0) \end{cases} \tag{5.5}$$

where r_0 is the separatrix radius, $R = (X^2 + (Y - u\tau)^2)^{1/2}$, $A = -(u+\nu_0)r_0/k^2 J_1(kr_0)$, $B = ur_0/K_1(pr_0)$, $\alpha = u + (u+\nu_0)/k^2$, $p^2 = 1 + \nu_0/u$, and k is related to p by the continuity relation of the derivative $\partial\Psi/\partial R$ at $R = r_0$ as follows:

$$\frac{J_2(kr_0)}{J_1(kr_0)} = -\frac{kK_2(pr_0)}{pK_1(pr_0)}. \tag{5.6}$$

When we assume $\nu_0 = -0.1$, $u = 0.2$ and $r_0 = 1$, the modon in the new coordinates $(\boldsymbol{X},\tau)$ is shown in Fig. 1. Using eq. (5.3), the modon in Fig. 1 is transformed to the profile of ϕ shown in Fig. 2.

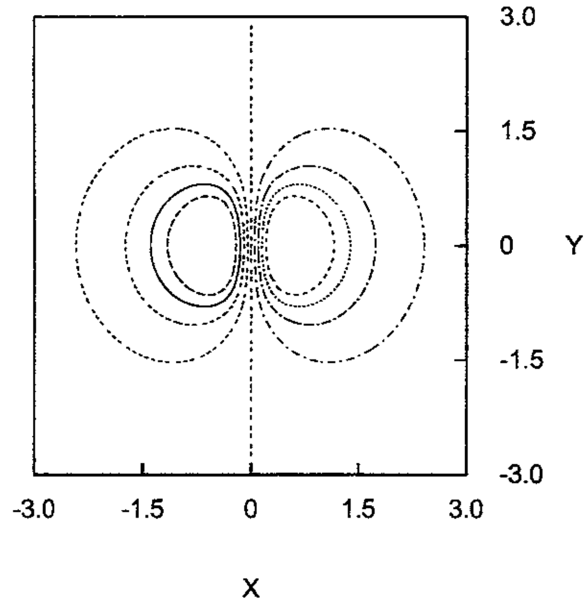

Fig. 1. A plot of Ψ for the modon, where $\nu_0 = -0.1$, $u = 0.2$ and $r_0 = 1$ in the dimensionless coordinates system. The interval of contour lines is 0.02 ranging from -0.16 to 0.16. The structure of dipole vortex is antisymmetric with respect to X and the vortex on the left hand side has a negative peak. Propagating velocity u is positive in the y direction and the negative equilibrium density gradient ν_0.

Comparing the new profile with the original modon shown in Fig. 1, we find out that the distortion of the modified modon in Fig. 2 is caused by the effect of the polarization drift, because the transformation of contour lines is perpendicular to the $E \times B$ drift which is along the lines in Fig. 1, and proportional to the gradient of ϕ approximately.

5.2 Example 2: Rossby Vortices in the Long Wavelength Ordering

The transformation of variables in the long wavelength ordering for nonlinear Rossby vortices has been discussed by Orito, Sato and Irie.[7]. In this section we will treat the transformation of variables up to the second order. The lowest and the second order terms of the velocity in this ordering are $\boldsymbol{v}_l$ and $\boldsymbol{v}_\beta$ in eq. (3.6), respectively. It is clear that the transformation of variables is given by

$$\begin{cases} \boldsymbol{\xi} = \beta_1 x^2 / 2\hat{\boldsymbol{x}}, \\ \Psi = h. \end{cases} \tag{5.7}$$

If the potential Ψ is known, The vertical fluid displacement is written as

$$h = \Psi(\boldsymbol{x} + \beta_1 x^2 / 2\hat{\boldsymbol{x}}, t). \tag{5.8}$$

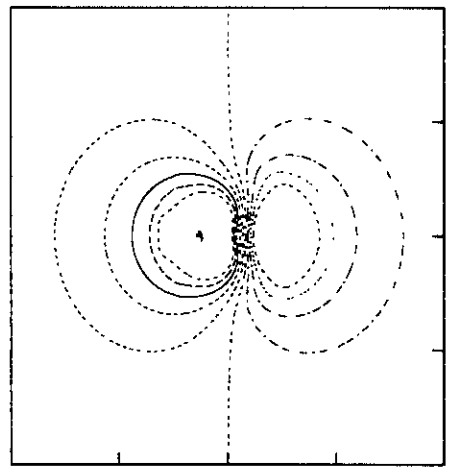

Fig 2 An electrostatic potential ϕ of eq. (5.3) for the dipole vortex solution Ψ. The interval of contours and parameters are the same as them in Fig. 1. The interval of contour lines is 0.04 ranging from -0.2 to 0.2.

Since the Coriolis parameter β_1 is always positive, the profile of h is necessarily distorted toward south comparing with the one of Ψ.

The potential vorticity up to the second order in ϵ is written as

$$q(\boldsymbol{X},\tau) = \nabla'^2\Psi - \Psi + \beta_1 X + \Psi^2 \\ - \beta_1 X\Psi + \frac{\beta_2 - \beta_1^2}{2}X^2. \tag{5.9}$$

In the stationary condition $\partial/\partial\tau = -u\partial/\partial X$, we derive a equation similar to eq. (3.14),

$$\nabla'^2\Psi + \lambda\Psi^2 + \gamma X\Psi - \kappa^2\Psi = 0, \tag{5.10}$$

where parameters λ, γ and κ have the same definitions as in eq. (3.14).

Although monopole solutions of eq. (5.10) are not valid for all space as we discussed in Sec. 3, we apply the transformation of variables (5.7) to the monopole solution in order to investigate its effect. For example, Orito, Sato and Irie derived a monopole solution in the region $r \sim \epsilon$,

$$\Psi(R) = \frac{a\kappa^2}{\lambda}[\mathrm{sech}(b\kappa R)]^{1/b}, \tag{5.11}$$

where $R = |\boldsymbol{X}|$, $a = 1 + \sqrt{3/2}$ and $b = \sqrt{3/8}$.[7,8] Substituting eq. (5.11) into eq. (5.8), we find out that the profile of h is distorted toward south as shown in Fig. 3. Since the profile of the

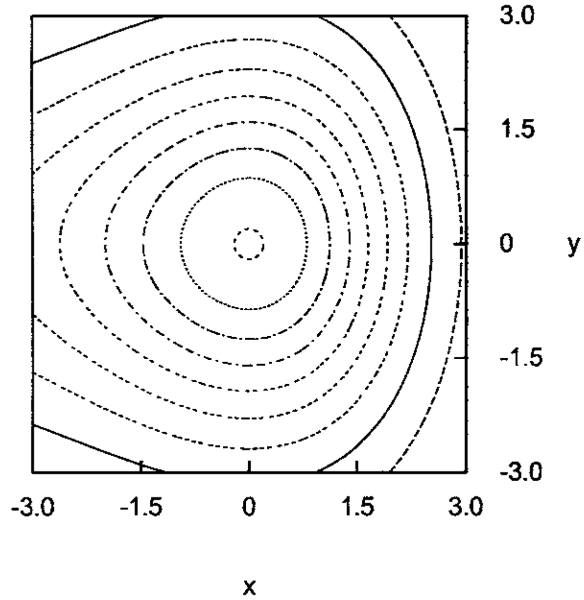

Fig. 3. A depth of fluid h of eq. (5.13), where $\beta_1 = 0.1$, $\beta_2 = -0.0016$, $u = 0.2$ and $r_0 = 1$. The interval of contour lines is 0.1 ranging from 0.2 to 1.0. The origin is located in latitude θ_0 N., which $\tan\theta_0 = 0.16$. The x-axis is toward north and y-axis west.

monopole solution (5.11) is circular, the distortions of contour lines owe to only the effect of $\boldsymbol{v}_\beta$ and this result agrees with our prediction. This distortion depends on the Coriolis parameter β_1 which is proportional to $\cot\theta_0$, so that the magnitude of distortion varies with the latitude θ_0.

5.3 Example 3: Rossby Vortices in the Short Wavelength Ordering

In the short wavelength ordering, the second order terms of the velocity are $\boldsymbol{v}_\beta$ (3.8) and $\boldsymbol{v}_h$ (3.9). As this is a hybrid case of examples 1 and 2, we obtain the transformation of variables, as follows:

$$\begin{cases} \boldsymbol{\xi} = \nabla h + \beta x^2/2\hat{\boldsymbol{x}}, \\ \Psi = h + \dfrac{1}{2}(\nabla h)^2. \end{cases} \tag{5.12}$$

The vertical fluid displacement h is written as

$$\begin{aligned} h(\boldsymbol{x},t) = \Psi(&\boldsymbol{x} + \nabla\Psi(\boldsymbol{x}) + \beta_1 x^2/2, t) \\ &+ \frac{1}{2}[\nabla\Psi(\boldsymbol{x})]^2. \end{aligned} \tag{5.13}$$

The potential vorticity in the lowest order is given by

$$q(\boldsymbol{X},\tau) = \nabla'^2\Psi - \Psi + \beta_1 X. \tag{5.14}$$

Notice that eqs. (5.4) and (5.14) are of the same form. When the solution Ψ is the modon as eq. (5.5), the fluid displacement h has the profile shown in Fig. 4. The Coriolis parameter β_1 in Fig. 4

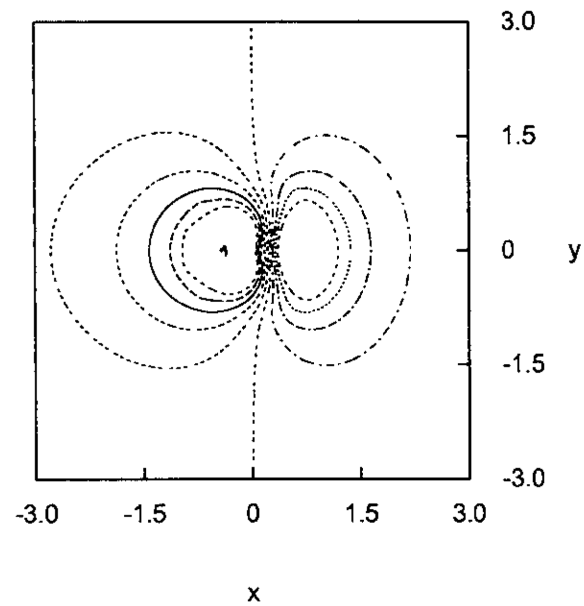

Fig. 4. A depth of fluid h of eq. (5.13), where parameters are same as them in Fig. 3 and correspond to in Fig. 1 for the drift wave. The interval of contour lines is 0.04 ranging from -0.2 to 0.2.

corresponding to the negative equilibrium density gradient $-\nu_0$ is chosen to be the same value as $-\nu_0$ in Figs. 1 and 2. If the second order velocity was $\boldsymbol{v}_h$ (3.9), then Fig. 4 would be identical to Fig. 2. However, the correct second order velocity is $\boldsymbol{v}_\beta + \boldsymbol{v}_h$, the distortion in Fig. 4 is enhanced as in Fig. 2 because of the effect of $\boldsymbol{v}_\beta$.

§6. Discussion and Conclusion

In Sec. 4, it has been shown how to obtain a transformation of variables in general from the conservation law of the potential vorticity. In the application to any problems, we need two conditions in order that the convective derivative $\boldsymbol{v} \cdot \nabla q$ can be transformed to the Poisson bracket form $\{\Psi, q\}'$ as in eq. (4.4). At first the velocity in the lowest ordering has to be described by a stream function, that is $\boldsymbol{v}_1 = \hat{\boldsymbol{z}} \times \nabla \psi_1$. The second condition is that the second order terms of the velocity need to satisfy eq. (4.7). In practical problems it is difficult to satisfy these conditions, but we have shown that they are successfully satisfied in three examples in Sec. 5. Especially, the drift wave case is a typical example by the following reason. Choosing $\psi_2 = \boldsymbol{\xi}^2/2$, the second condition (4.7) can be written $\boldsymbol{v}_2 = -d\boldsymbol{\xi}/dt$. The second order velocity $\boldsymbol{v}_2$ for drift vortices, i.e. a polarization drift velocity, is the negative time derivative of gradient ϕ, $\boldsymbol{v}_p = -d\nabla\phi$. Therefore, the polarization drift velocity satisfies eq. (4.7) automatically. On the other hand, the Rossby vortices case in the long wavelength ordering is a different situation, because the new coordinate vector $\boldsymbol{X}$ is defined by $\nabla\boldsymbol{\xi} = \beta_1 x$.

In these examples 5.1-5.3, we illustrated distorted dipole or monopole vortices. The transformation of variables obtained in various case in Sec. 5 may be applied to not only modons and a monopole vortex but also other solutions in the new coordinates $(\boldsymbol{X}, \tau)$. Any solutions obtained in this procedure have profiles distorted by the effect of higher order terms which are $\boldsymbol{v}_p$ in plasmas or $\boldsymbol{v}_\beta$ and $\boldsymbol{v}_h$ in geostrophic flows.

Here we mention briefly about the drift vortex in the long wavelength ordering which have not been discussed. The transformation of variables is identical to the case of the short wave length ordering. However, it is negligible because the effect of the polarization drift depends on the third order terms and there is no second order terms of velocity in this ordering.

In conclusion, we have shown a technique to get rid of complicated nonlinear terms and higher derivatives in the nonlinear equations for the drift and Rossby vortices. It makes the nonlinear analysis extremely transparent as compared with the straightforward calculation. Since all of solutions in three examples are stationary solutions, these profiles must propagate stably as modons do. An examination of this result by numerical simulation is a future subject.

Acknowledgements

The author is grateful to Professor Tadatsugu Hatori of National Institute for Fusion Science and Professor Masatomo Sato of Nihon University for valuable discussions.

1) A. Hasegawa and K. Mima: Phys. Fluids **21** (1978) 87.
2) V. D. Larichev and G. M. Reznik: Dokl. Akad. Nauk SSSR **231** (1976) 1077.
3) J. D. Meiss and W. Horton: Phys. Fluids **26** (1983) 990.
4) H. Moriguchi and K. Nozaki: J. Phys. Soc. Jpn. **61** (1992) 117.
5) X. N. Su, P. N. Yushmanov, J. Q. Dong and W. Horton: Phys. Plasmas 1 (1994) 1905.
6) J. G. Charney: Geophys. Public. Kosjones Nors. Videnshap. Akad. Oslo **17** (1948) 3.
7) K. Orito, M. Sato and H. Irie: J. Phys. Soc. Jpn. **64** (1995) 1874.
8) S. Horihata and M. Sato: J. Phys. Soc. Jpn. **56** (1990) 2611.
9) J. Nycander: *Nonlinear World*, ed. V. G. Bar'yakhtar (World Scientific, Singapore, 1989) Vol. 2, p. 933.
10) J. Nycander: Phys. Rev. Lett. **67** (1991) 1671

Recent Issues of NIFS Series

NIFS-377 J. Uramoto,
Extraction of Negative Pionlike Particles from a H2 or D2 Gas Discharge Plasma in Magnetic Field; Sep. 1995

NIFS-378 K. Akaishi,
Theoretical Consideration for the Outgassing Characteristics of an Unbaked Vacuum System; Oct. 1995

NIFS-379 H. Shimazu, S. Machida and M. Tanaka,
Macro-Particle Simulation of Collisionless Parallel Shocks; Oct. 1995

NIFS-380 N. Kondo and Y. Kondoh,
Eigenfunction Spectrum Analysis for Self-organization in Dissipative Solitons; Oct. 1995

NIFS-381 Y. Kondoh, M. Yoshizawa, A. Nakano and T. Yabe,
Self-organization of Two-dimensional Incompressible Viscous Flow in a Friction-free Box; Oct. 1995

NIFS-382 Y.N. Nejoh and H. Sanuki,
The Effects of the Beam and Ion Temperatures on Ion-Acoustic Waves in an Electron Beam-Plasma System; Oct. 1995

NIFS-383 K. Ichiguchi, O. Motojima, K. Yamazaki, N. Nakajima and M. Okamoto
Flexibility of LHD Configuration with Multi-Layer Helical Coils; Nov. 1995

NIFS-384 D. Biskamp, E. Schwarz and J.F. Drake,
Two-dimensional Electron Magnetohydrodynamic Turbulence; Nov. 1995

NIFS-385 H. Kitabata, T. Hayashi, T. Sato and Complexity Simulation Group,
Impulsive Nature in Collisional Driven Reconnection; Nov. 1995

NIFS-386 Y. Katoh, T. Muroga, A. Kohyama, R.E. Stoller, C. Namba and O. Motojima,
Rate Theory Modeling of Defect Evolution under Cascade Damage Conditions:The Influence of Vacancy-type Cascade Remnants and Application to the Defect Production Chracterization by Microstructural Analysis; Nov. 1995

NIFS-387 K. Araki. S. Yanase and J. Mizushima,
Symmetry Breaking by Differential Rotation and Saddle-node Bifurcation of the Thermal Convection in a Spherical Shell; Dec. 1995

NIFS-388 V.D. Pustovitov,
Control of Pfirsch-Schlüter Current by External Poloidal Magnetic Field in Conventional Stellarators: Dec. 1995

NIFS-389 K. Akaishi,
On the Outgassing Rate Versus Time Characteristics in the Pump-down of an Unbaked Vacuum System; Dec. 1995

NIFS-390 K.N. Sato, S. Murakami, N. Nakajima, K. Itoh,
Possibility of Simulation Experiments for Fast Particle Physics in Large Helical Device (LHD); Dec. 1995

NIFS-391 W.X.Wang, M. Okamoto, N. Nakajima, S. Murakami and N. Ohyabu,
A Monte Carlo Simulation Model for the Steady-State Plasma in the Scrape-off Layer; Dec. 1995

NIFS-392 Shao-ping Zhu, R. Horiuchi, T. Sato and The Complexity Simulation Group,
Self-organization Process of a Magnetohydrodynamic Plasma in the Presence of Thermal Conduction; Dec. 1995

NIFS-393 M. Ozaki, T. Sato, R. Horiuchi and the Complexity Simulation Group
Electromagnetic Instability and Anomalous Resistivity in a Magnetic Neutral Sheet; Dec. 1995

NIFS-394 K. Itoh, S.-I Itoh, M. Yagi and A. Fukuyama,
Subcritical Excitation of Plasma Turbulence; Jan. 1996

NIFS-395 H. Sugama and M. Okamoto, W. Horton and M. Wakatani,
Transport Processes and Entropy Production in Toroidal Plasmas with Gyrokinetic Eletromagnetic Turbulence; Jan. 1996

NIFS-396 T. Kato, T. Fujiwara and Y. Hanaoka,
X-ray Spectral Analysis of Yohkoh BCS Data on Sep. 6 1992 Flares - Blue Shift Component and Ion Abundances -; Feb. 1996

NIFS-397 H. Kuramoto, N. Hiraki, S. Moriyama, K. Toi, K. Sato, K. Narihara, A. Ejiri, T. Seki and JIPP T-IIU Group,
Measurement of the Poloidal Magnetic Field Profile with High Time Resolution Zeeman Polarimeter in the JIPP T-IIU Tokamak; Feb. 1996

NIFS-398 J.F. Wang, T. Amano, Y. Ogawa, N. Inoue,
Simulation of Burning Plasma Dynamics in ITER; Feb. 1996

NIFS-399 K. Itoh, S-I. Itoh, A. Fukuyama and M. Yagi,
Theory of Self-Sustained Turbulence in Confined Plasmas; Feb. 1996

NIFS-400 J. Uramoto,
A Detection Method of Negative Pionlike Particles from a H2 Gas Descharge Plasma; Feb. 1996

NIFS-401 K.Ida, J.Xu, K.N.Sato, H.Sakakita and JIPP TII-U group,
Fast Charge Exchange Spectroscopy Using a Fabry-Perot Spectrometer

in the JIPP TII-U Tokamak; Feb. 1996

NIFS-402 T. Amano,
Passive Shut-Down of ITER Plasma by Be Evaporation; Feb. 1996

NIFS-403 K. Orito,
A New Variable Transformation Technique for the Nonlinear Drift Vortex; Feb. 1996

NIFS-404 T. Oike, K. Kitachi, S. Ohdachi, K. Toi, S. Sakakibara, S. Morita, T. Morisaki, H. Suzuki, S. Okamura, K. Matsuoka and CHS group; *Measurement of Magnetic Field Fluctuations near Plasma Edge with Movable Magnetic Probe Array in the CHS Heliotron/Torsatron*; Mar. 1996

NIFS-405 S.K. Guharay, K. Tsumori, M. Hamabe, Y. Takeiri, O. Kaneko, T. Kuroda,
Simple Emittance Measurement of H- Beams from a Large Plasma Source; Mar. 1996

NIFS-406 M. Tanaka and D. Biskamp,
Symmetry-Breaking due to Parallel Electron Motion and Resultant Scaling in Collisionless Magnetic Reconnection; Mar. 1996

NIFS-407 K. Kitachi, T. Oike, S. Ohdachi, K. Toi, R. Akiyama, A. Ejiri, Y. Hamada, H.Kuramoto, K. Narihara, T. Seki and JIPP T-IIU Group,
Measurement of Magnetic Field Fluctuations within Last Closed Flux Surface with Movable Magnetic Probe Array in the JIPP T-IIU Tokamak; Mar. 1996

NIFS-408 K. Hirose, S. Saito and Yoshi.H. Ichikawa
Structure of Period-2 Step-1 Accelerator Island in Area Preserving Maps; Mar. 1996

NIFS-409 G.Y.Yu, M. Okamoto, H. Sanuki, T. Amano,
Effect of Plasma Inertia on Vertical Displacement Instability in Tokamaks; Mar. 1996

NIFS-410 T. Yamagishi,
Solution of Initial Value Problem of Gyro-Kinetic Equation; Mar. 1996

NIFS-411 K. Ida and N. Nakajima,
Comparison of Parallel Viscosity with Neoclassical Theory; Apr. 1996

NIFS-412 T. Ohkawa and H. Ohkawa,
Cuspher, A Combined Confinement System; Apr. 1996

NIFS-413 Y. Nomura, Y.H. Ichikawa and A.T. Filippov,
Stochasticity in the Josephson Map; Apr. 1996

NIFS-414 J. Uramoto,

Production Mechanism of Negative Pionlike Particles in H_2 Gas Discharge Plasma; Apr. 1996

NIFS-415 A. Fujisawa, H. Iguchi, S. Lee, T.P. Crowley, Y. Hamada, S. Hidekuma, M. Kojima,
Active Trajectory Control for a Heavy Ion Beam Probe on the Compact Helical System; May 1996

NIFS-416 M. Iwase, K. Ohkubo, S. Kubo and H. Idei
Band Rejection Filter for Measurement of Electron Cyclotron Emission during Electron Cyclotron Heating; May 1996

NIFS-417 T. Yabe, H. Daido,T. Aoki, E. Matsunaga and K. Arisawa,
Anomalous Crater Formation in Pulsed-Laser-Illuminated Aluminum Slab and Debris Distribution; May 1996

NIFS-418 J. Uramoto,
Extraction of K^- Mesonlike Particles from a D_2 Gas Discharge Plasma in Magnetic Field; May 1996

NIFS-419 J. Xu, K. Toi, H. Kuramoto, A. Nishizawa, J. Fujita, A. Ejiri, K. Narihara, T. Seki, H. Sakakita, K. Kawahata, K. Ida, K. Adachi, R. Akiyama, Y. Hamada, S. Hirokura, Y. Kawasumi, M. Kojima, I. Nomura, S. Ohdachi, K.N. Sato
Measurement of Internal Magnetic Field with Motional Stark Polarimetry in Current Ramp-Up Experiments of JIPP T-IIU; June 1996

NIFS-420 Y.N. Nejoh,
Arbitrary Amplitude Ion-acoustic Waves in a Relativistic Electron-beam Plasma System; July 1996

NIFS-421 K. Kondo, K. Ida, C. Christou, V.Yu.Sergeev, K.V.Khlopenkov, S.Sudo, F. Sano, H. Zushi, T. Mizuuchi, S. Besshou, H. Okada, K. Nagasaki, K. Sakamoto, Y. Kurimoto, H. Funaba, T. Hamada, T. Kinoshita, S. Kado, Y. Kanda, T. Okamoto, M. Wakatani and T. Obiki,
Behavior of Pellet Injected Li Ions into Heliotron E Plasmas; July 1996

NIFS-422 Y. Kondoh, M. Yamaguchi and K. Yokozuka,
Simulations of Toroidal Current Drive without External Magnetic Helicity Injection; July 1996

NIFS-423 Joong-San Koog,
Development of an Imaging VUV Monochromator in Normal Incidence Region; July 1996

NIFS-424 K. Orito,
A New Technique Based on the Transformation of Variables for Nonlinear Drift and Rossby Vortices; July 1996